A Lecture on Selective RF-pulses in MRI

Charles L. Epstein*

February 11, 2003

1 Introduction

We describe the notion of selective excitation and explain how the Bloch equation is used to design selective RF-pulses. In our discussion we concentrate on the Fourier method. This is an approximate method which uses a further simplification of the Bloch equation.

2 The Bloch Equation

The Bloch equation is a good empirical model for the behavior of either a single proton spin in a magnetic field, or for the bulk magnetization of an isochromat. It is the latter interpretation which is more useful in the present discussion. We ignore relaxation effects, so our analysis is only meaningful for times which are short compared to T_1 and T_2. If $\boldsymbol{M}$ is the magnetization and $\boldsymbol{B}$ is the magnetic field then Bloch's equation states that

$$\frac{d\boldsymbol{B}}{dt} = \gamma(1+\sigma)\boldsymbol{B} \times \boldsymbol{M}. \tag{1}$$

Here γ is the gyromagnetic ratio (≈ 4.26MHz/Tesla) and σ is the chemical shift. Throughout this discussion we let $\sigma = 0$. A solution to (1) is specified by fixing the value of $\boldsymbol{M}$ at one time. In most of the subsequent discussion we label the t-axis

*Address: Department of Mathematics, and LSNI, HUP, University of Pennsylvania, Philadelphia, PA. E-mail: cle@math.upenn.edu

so that the initial data is given at $t = 0$, e.g., $\boldsymbol{M}(0) = \boldsymbol{M}_0$. In MR applications $\boldsymbol{B}$ is of the form

$$\boldsymbol{B} = \boldsymbol{B}_0 + \boldsymbol{B}_1$$

where $\boldsymbol{B}_0$ is the background field and $\boldsymbol{B}_1$ is the RF-field. The background field is of the form

$$\boldsymbol{B}_0 = \boldsymbol{B}_{00} + G(\boldsymbol{r})\hat{\boldsymbol{z}},$$

where $\boldsymbol{B}_{00}$ is a very large, uniform, time independent background field in the direction $\hat{\boldsymbol{z}}$, and $G(\boldsymbol{r})\hat{\boldsymbol{z}}$ is a spatially varying gradient field. There are of course gradient components in the $\hat{\boldsymbol{x}}$- and $\hat{\boldsymbol{y}}$-directions as well. Since they have such a small effect on the evolution of $\boldsymbol{M}$, they can safely be ignored. The gradient is assumed to be a function of the form $g(\boldsymbol{r} \cdot \boldsymbol{v})$; indeed it is usually assumed to be simply $c\boldsymbol{r} \cdot \boldsymbol{v}$. In the latter case we say that there is a *linear gradient* in the $\boldsymbol{v}$-direction. The $\boldsymbol{B}_1$-field is a time dependent field of the form

$$\boldsymbol{B}_1 = e^{i\omega_0 t}(b_x(t), b_y(t), 0),$$

here ω_0 is the reference Larmor frequency (usually the Larmor frequency of the $\boldsymbol{B}_{00}$ part of the background field).

Before studying selective excitation, we recall some basic facts about solutions to the Bloch equation.

Proposition 1. *Suppose that $\boldsymbol{v}_1(t)$ and $\boldsymbol{v}_2(t)$ are solutions to* (1). *Then $a\boldsymbol{v}_1 + b\boldsymbol{v}_2$ is also a solution, for any constants a, b and the inner product $\langle \boldsymbol{v}_1(t), \boldsymbol{v}_2(t)\rangle$ is independent of t.*

Proof. The linearity is immediate from the form of the equation. To prove the second statement we differentiate

$$\begin{aligned}\frac{d}{dt}\langle \boldsymbol{v}_1(t), \boldsymbol{v}_2(t)\rangle &= \langle \frac{d}{dt}\boldsymbol{v}_1(t), \boldsymbol{v}_2(t)\rangle + \langle \boldsymbol{v}_1(t), \frac{d}{dt}\boldsymbol{v}_2(t)\rangle \\ &= \langle \boldsymbol{B} \times \boldsymbol{v}_1(t), \boldsymbol{v}_2(t)\rangle + \langle \boldsymbol{v}_1(t), \boldsymbol{B} \times \boldsymbol{v}_2(t)\rangle.\end{aligned} \tag{2}$$

The proof is completed using the standard fact about cross products

$$\langle \boldsymbol{v}_3 \times \boldsymbol{v}_1(t), \boldsymbol{v}_2(t)\rangle = -\langle \boldsymbol{v}_1(t), \boldsymbol{v}_3 \times \boldsymbol{v}_2(t)\rangle.$$

□

Exercise 1. Prove the identity for the cross product.

The first claim is the proposition is usually phrased as the statement that "the Bloch equation is a linear ODE." Because (1) is linear, there is a 3×3- matrix valued function $U_0(t)$ such that $U_0(0) = \mathrm{Id}_3$ and

$$\boldsymbol{M}(t) = U_0(t)\boldsymbol{M}_0.$$

The proposition implies that $U_0(t)$ is a rotation matrix, that is

$$U_0^\dagger(t)U_0(t) = U_0(t)U_0^\dagger(t) = \mathrm{Id}_3\,.$$

In MR we usually discuss the Bloch equation in the *rotating frame*. If $\boldsymbol{B}_1$ and $G\hat{\boldsymbol{z}}$ are both zero then the solution operator for (1) takes a very simple form

$$U_0^{\mathrm{res}}(t) = \begin{pmatrix} \cos(\omega_0 t) & -\sin(\omega_0 t) & 0 \\ \sin(\omega_0 t) & \cos(\omega_0 t) & 0 \\ 0 & 0 & 1 \end{pmatrix}.$$

This is a rotation, about the $\hat{\boldsymbol{z}}$-axis, through the angle $\omega_0 t$. Because $\boldsymbol{B}_1$ and G are small perturbations, it makes sense to write

$$U_0(t) = U_0^{\mathrm{res}}(t)V(t).$$

To that end we write $\boldsymbol{M}(t) = U_0^{\mathrm{res}}(t)\boldsymbol{\mu}(t)$. Larmor's theorem states that if $\boldsymbol{M}$ solves (1) then $\boldsymbol{\mu}$ solves

$$\frac{d\boldsymbol{\mu}}{dt} = \gamma \boldsymbol{B}_{\text{eff}} \times \boldsymbol{\mu}, \tag{3}$$

where $\boldsymbol{B}_{\text{eff}}$ is the effective magnetic field. It is given by

$$\boldsymbol{B}_{\text{eff}} = [U_0^{\mathrm{res}}(t)]^{-1}\boldsymbol{B} + \frac{1}{\gamma}\boldsymbol{\Omega},$$

where the laboratory frame is related to the rotating frame by a rotation with axis $\boldsymbol{\Omega}$. Usually $\boldsymbol{\Omega}$ is just a constant multiple of $\hat{\boldsymbol{z}}$, though this is by no means necessary for the truth of Larmor's theorem.

The reason for using the rotating frame is to simplify the form of $\boldsymbol{B}$ and thereby the form of the solution. Usually it is assumed that

$$\boldsymbol{B}_{\text{eff}} = \gamma^{-1}(\alpha(t), \beta(t), f),$$

where f is independent of t. In applications to MR, f assumes a range of values $[-f_0, f_0]$. For a gradient of the form $(g\boldsymbol{r} \cdot \boldsymbol{v})\hat{\boldsymbol{z}}$, each value of f corresponds to a plane passing through the field-of-view, i.e., the set of $\boldsymbol{r}$ such that $g\boldsymbol{r} \cdot \boldsymbol{v} = f$. Generally f is called the *resonance offset* or *offset frequency*. The complex valued function $\alpha(t) + i\beta(t)$ is called the *RF-envelope*

3 The Problem of Selective Pulse Design

Writing out the Bloch equation in the rotating frame gives

$$\frac{d}{dt}\begin{pmatrix}\mu_1\\ \mu_2\\ \mu_3\end{pmatrix} = \begin{pmatrix}0 & f & -\beta\\ -f & 0 & \alpha\\ \beta & -\alpha & 0\end{pmatrix}\begin{pmatrix}\mu_1\\ \mu_2\\ \mu_3\end{pmatrix}. \tag{4}$$

We now think of the solution operator V as a function of the pair $(f;t)$. The basic problem of selective pulse design is the following: we specify a unit vector valued function $\boldsymbol{\mu}_{\text{ss}}(f)$ and look for a pair of functions $(\alpha(t),\beta(t))$ so that

$$V(f;T)\hat{\boldsymbol{z}} = \boldsymbol{\mu}_{\text{ss}}(f) \text{ for } f \in [-f_0, f_0]. \tag{5}$$

In other words we look for an RF-envelope so that, as a function of the offset frequency, the solution of (4), with initial data $\hat{\boldsymbol{z}}$, is given, at time T, by $\boldsymbol{\mu}_{\text{ss}}(f)$. The function $\boldsymbol{\mu}_{\text{ss}}(f)$ is called the *magnetization profile*. A typical example is

$$\boldsymbol{\mu}_{\text{ss}}(f) = \begin{cases}(\sin\psi, 0, \cos\psi) & \text{for } f \in [f_1, f_2]\\ (0,0,1) & \text{for } f \notin [f_1, f_2].\end{cases} \tag{6}$$

In this case ψ is called the *flip angle*. In most applications $[f_1, f_2]$ is a small subinterval of $[-f_0, f_0]$.

This looks like a pretty odd question to ask about an ODE: We are looking for *coefficients* $\alpha(t),\beta(t)$ so that, for a given initial condition, the solution at a specified time T, will have a certain dependence on the auxiliary parameter f. The mapping between $(\alpha(t),\beta(t))$ and $V(f;T)\hat{\boldsymbol{z}}$ is highly nonlinear (this is what is meant in the MR literature when it is stated that the "Bloch equation is nonlinear"). Nonetheless, this problem has been analyzed extensively by both mathematicians and physicists and admits of several different *exact* solutions. We briefly return to this at the end of the lecture. We now classical the classical, *approximate* approach to selective pulse design, often called the *Fourier method*.

Using this method, we can design reasonably good pulses with small flip angles. If the flip angle is small then μ_3 deviates very little from its initial value of 1. Because, for $|\psi|$ close to zero, $\sin\psi$ tends to be much larger than $(1-\cos\psi)$. (Can you explain why?), even though μ_3 stays very close to 1, $|\mu_1 + i\mu_2|$ can get to be reasonably large. For example

$$1 - \cos\frac{\pi}{6} = .13 \text{ whereas } \sin\frac{\pi}{6} = .5.$$

The size of (μ_1,μ_2) is very important in MRI, because the strength of the measurable signal is proportional to $\|(\mu_1,\mu_2)\|$.

4 The Fourier Method

To explain the Fourier method we need to rewrite the Bloch equation once again, this time using complex notation:

$$
\begin{aligned}
e^{-ift}\frac{d[e^{ift(\mu_1+i\mu_2)}]}{dt} &= i\mu_3(t)(\alpha(t)+i\beta(t))\\
\frac{d\mu_3}{dt} &= \beta\mu_1-\alpha\mu_2.
\end{aligned} \tag{7}
$$

The complex valued function $\mu_1 + i\mu_2$ is usually called the *transverse component* of the magnetization. If we suppose, for the moment, that we somehow know $\mu_3(t)$, for all t, then it is a simple matter to find $\mu_1 + i\mu_2$. Integrating the first equation in (7) gives:

$$
\mu_1(f;t) + i\mu_2(f;t) = ie^{-ift}\int_0^t e^{ifs}\mu_3(s)(\alpha(s)+i\beta(s))ds. \tag{8}
$$

In the small flip angle approximation, we just assume that $\mu_3 \equiv 1$. If $\alpha + i\beta$ is supported in $[0, T]$ then this implies that

$$
\mu_1(f;T) + i\mu_2(f;T) \approx ie^{-ifT}\int_0^T e^{ifs}(\alpha(s)+i\beta(s))ds. \tag{9}
$$

But for the multiplicative factor, ie^{-ifT}, the transverse magnetization at time T, $\mu_1(f;T)+i\mu_2(f;T)$, is the 2π times the inverse Fourier transform of $\alpha+i\beta$. Thus, in the small flip angle approximation, the shape of the RF-envelope is determined by taking the Fourier transform of $\boldsymbol{\mu}_{\text{ss}}$. Let's consider an example.

Definition 1. For an interval $[a, b]$ the *characteristic function* of $[a, b]$, denoted by $\chi_{[a,b]}(x)$ is defined by

$$
\chi_{[a,b]}(x) = \begin{cases} 1 & \text{if } a \leq x \leq b, \\ 0 & \text{otherwise.} \end{cases}
$$

If $\boldsymbol{\mu}_{\text{ss}}$ is given by (6), with $f_1 = -w$, $f_2 = w$ then, ignoring the phase factor in (9), we would expect

$$
\alpha + i\beta = c(\psi)\frac{\sin(wt)}{t},
$$

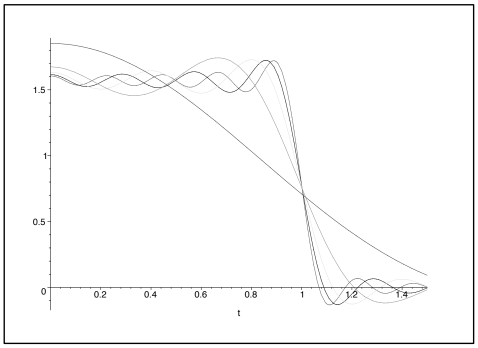

(a) The inverse Fourier transform of several truncations of the sinc function.

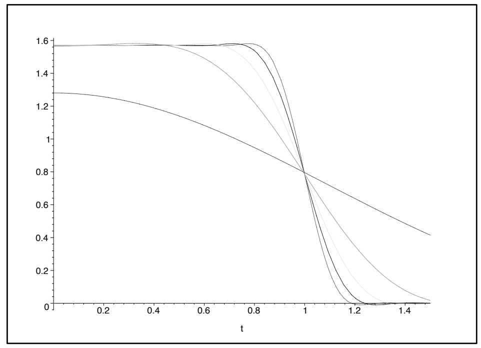

(b) The result of using $\cos^2$ to truncate.

Figure 1. The inverse Fourier transforms of various windowed sinc functions.

where $c(\psi)$ is a constant proportional to $\sin\psi$. This function is not supported in a finite interval. In practice we use a finite part of this function, for example a function of the form

$$c(\psi)\chi_{[-\frac{n\pi}{w},\frac{n\pi}{w}]}(t-\frac{n\pi}{w})\frac{\sin(wt-n\pi)}{t-\frac{n\pi}{w}}. \tag{10}$$

We have also shifted the time origin so the function is nonzero in the interval $[0,T]$, with $T=\frac{2n\pi}{w}$. Observe that T, the duration of the pulse, is related to w, the bandwidth of the excitation. Plugging this form into (9) gives

$$\mu_1(f;T)+i\mu_2(f;T)\approx ie^{-\frac{ifT}{2}}r_n(f), \tag{11}$$

where $r_n(f)$ is an approximation to $\sin\psi\chi_{[-w,w]}(f)$. To avoid Gibbs oscillations, we often multiply the function in (10) by a function like $\cos^2(\frac{wt}{2n}-\frac{\pi}{2})$. Figure 1(a) show the inverse Fourier transforms of several different truncations of the sinc function. As we use more and more lobes the approximation to the sharp window improves. In Figure 1(b) we show the result of using the $\cos^2$ to get a smoother cutoff. The ripple and overshoot are now absent but the transition region is about twice as large.

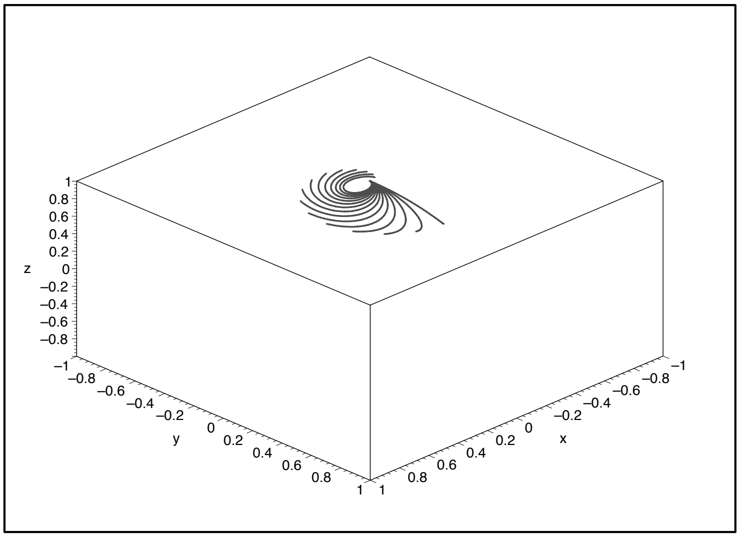

Figure 2. Solutions to the Bloch equation using a truncated sinc pulse and a range of offset frequencies.

5 Rephasing

For small flip angles, this gives a good approximation to $|\boldsymbol{\mu}_{\text{ss}}(f)|$, however we still have to deal with the overall phase $e^{-\frac{ifT}{2}}$. The second part of pulse design involves removing such phase errors in order to obtain spins which are aligned across the selected slice. Because of its simple linear dependence on f, this phase can be removed by simply reversing the direction of $\boldsymbol{B}_0$-gradient and allowing the spins to freely precess for an additional $\frac{T}{2}$ units of time. This is called *rephasing*; it is an essential part of the design of selective RF-pulse. After the rephasing period we will have achieved what we set out to do. Figure 2 shows trajectories obtained by solving the Bloch equation with a truncated sinc pulse. The different trajectories correspond to different offset frequencies. Observe how, as predicted, the endpoint rotates about the origin as the offset frequency increases. This demonstrates why it is necessary to rephase the magnetization after the RF-pulse is applied.

Before going on to another topic it pays to note that we are not free to specify T, the duration of the pulse. In fact it is connected to the bandwidth of the excitation. If $\alpha(t) + i\beta(t)$ produces the excitation $\boldsymbol{\mu}_{\text{ss}}(f)$ then, for any positive λ, the RF-envelope $\lambda(\alpha(\lambda t) + i\beta(\lambda t))$ produces the excitation $\boldsymbol{\mu}_{\text{ss}}(\frac{f}{\lambda})$. This shows that the bandwidth (BW) is inversely proportional to the duration of the excitation. The energy and amplitude of the RF-envelope are proportional to BW.

6 Time Dependent Gradients

Using the linear approximation, (i.e. the assumption that $\mu_3 \equiv 1$) we can also analyze the case where the gradients depend on time. This is very useful in real applications, because it allows us to apply RF-fields while the gradient is ramping up and thereby shorten the overall time needed for slice selection. Here we allow f, the offset frequency to be a function of time. In this case, formula (8) is replaced by

$$\mu_1(f;T) + i\mu_2(f;T) = ie^{-i\int_0^T f(s)ds} \int\limits_0^T e^{i\int_0^t f(s)ds}(\alpha(t) + i\beta(t))dt. \tag{12}$$

Assume now that $f(s)$ can expressed in terms of the gradient by $f(s) = kg(s)$, where $k = \gamma z$. Therefore

$$\int\limits_0^t f(s)ds = k \int\limits_0^t g(s)ds.$$

So long as $g(s) > 0$ we can use

$$\tau(t) = \int\limits_0^t g(s)ds$$

as an integration variable. This gives an expression of the form

$$\mu_1(k;T) + i\mu_2(k;T) = ie^{-ik\tau(T)} \int\limits_0^{\tau(T)} e^{ik\tau}[\alpha(t(\tau)) + i\beta(t(\tau))]\frac{dt}{d\tau}d\tau. \tag{13}$$

We have again obtained what is essentially a Fourier transform relationship between the magnetization profile and the RF-envelope.

7 Examples

In this example we show that result of using a truncated sinc-pulse to obtain a flip angle of $\pi/32$ over a band of width 3000 Hz. The pulse we use in shown in

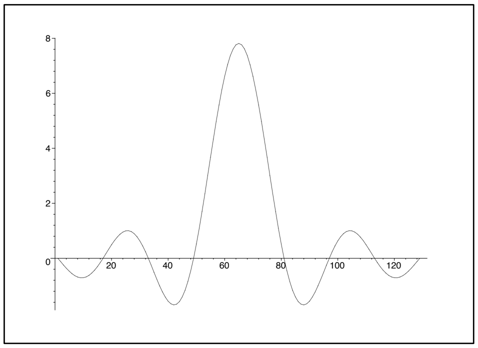

(a) A truncated $\frac{\pi}{32}$ sinc-pulse

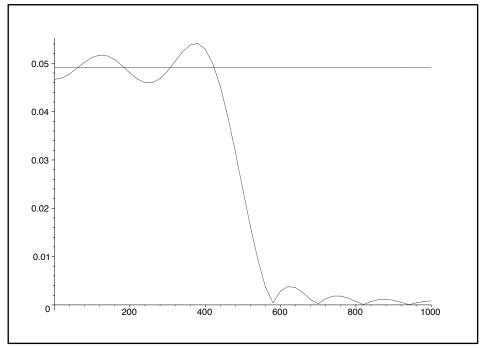

(b) The z-magnetization

Figure 3. A plot of a truncated $\frac{\pi}{32}$-sinc pulse and the z-component of the magnetization profile it produces.

Figure 3(a) and the z-component of the magnetization is shown in Figure 3(b). The excitation is essentially in the correct band, however there is a lot of ripple and overshoot. In Figure 4 we show a truncated $\frac{\pi}{2}$ sinc pulse and the magnetization it produces. The profile is similar to that in Figure 3(b). Most commercial MR imaging equipment actually use small modifications of these sinc pulses.

8 Higher Flip Angles

In practice the most common examples are pulses with flip angles of either $90°$ of $180°$. Because of the large flip angles, these are usually designed using a more accurate method than that outlined in the previous sections. There are two approaches to this problem. As both require mathematical techniques well beyond the Fourier transform, we will not attempt to explain them here but simply give references. The more widely used in the Shinnar-Le Roux or SLR method. This is very well explained in [1]. The other approach is via the Inverse Scattering Transform or IST. A preprint on this subject entitled *Minimum energy pulse synthesis via the inverse scattering transform* can be found at http://www.math.upenn.edu/˜cle/papers/. These two papers contain references to many of the important papers on RF-pulse design.

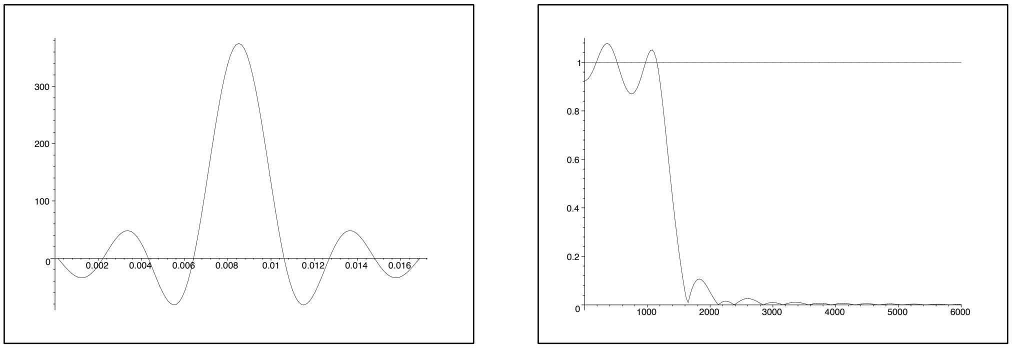

(a) A truncated $\frac{\pi}{32}$ sinc-pulse (b) The z-magnetization

Figure 4. A plot of a truncated $\frac{\pi}{2}$-sinc pulse and the z-component of the magnetization profile it produces.

9 RF-energy

We close this lecture with a relation between the total energy in RF-pulse and the magnetization profile it produces. If the RF-pulse is given by $e^{i\omega_0 t}(\alpha(t), \beta(t), 0)$, then the total energy of the pulse is given by a constant times the square norm of $\alpha + i\beta$:

$$\text{Total energy} = C_1 \int |\alpha(t) + i\beta(t)|^2 dt.$$

If it produces the magnetization profile $(\mu_1(f), \mu_2(f), \mu_3(f))$, then we have the relation

$$\int |\alpha(t) + i\beta(t)|^2 dt \geq C_2 \int \log \left[1 + \frac{|\mu_1 + i\mu_2|^2}{|1 + \mu_3|^2}(f) \right] df. \tag{14}$$

Here C_2 is a universal constant. The reason we have an inequality is because there are actually many RF-envelopes which will produce a given magnetization profile. This a reflection of the nonlinearity of the problem. On the other hand, there is a unique, minimum energy pulse, for which we get equality. We close the lecture by showing two examples of minimum energy pulses designed using the IST approach. Figure 5(a) shows the minimum energy $90°$ pulse and Figure 5(b) shows the magnetization it produces. Figure 6(a) shows the minimum energy pulse which produces the double band $90°$ excitation shown in Figure 6(b). In these magnetization profiles the x-component is the solid line, the y-component is

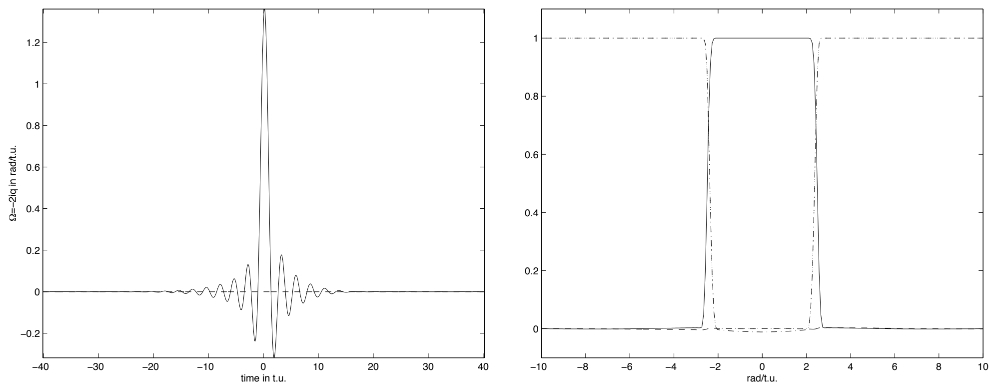

(a) The minimum energy 90° pulse.

(b) The rephased x, y, z components of the magnetization.

Figure 5. A plot of the minimum energy 90° pulse and the magnetization profile it produces.

the dashed line and the z-component is the dot-dashed line. The 90° pulse resembles a sinc function, though it should be noted that this function is not symmetric about $t = 0$.

References

[1] J. Pauly, P. Le Roux, D. Nishimura, and A. Macovski, *Parameter relations for the Shinnar-Le Roux selective excitation pulse design algorithm*, IEEE Trans. on Med. Imaging, 10 (1991), pp. 53–65.

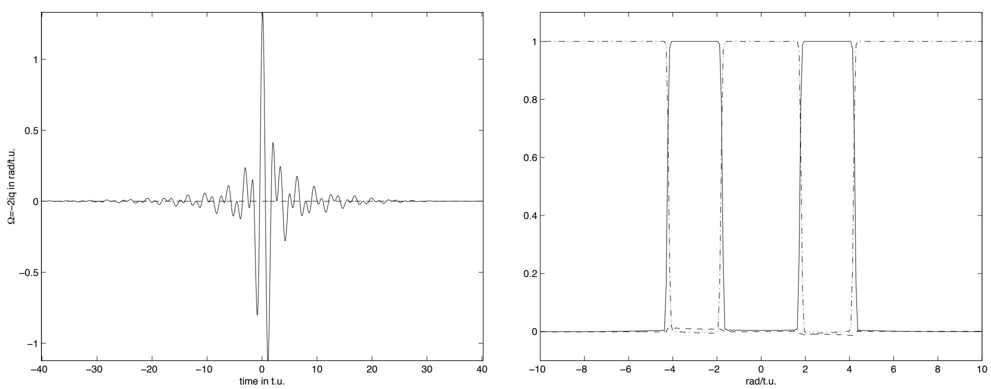

(a) The minimum energy, two band $90°$ pulse.

(b) The rephased x, y, z components of the magnetization.

Figure 6. A plot of the minimum energy two band $90°$ pulse and the magnetization profile it produces.